Role of Helical Wiggler on THz Radiation Generation from Free Electron Laser

A Dissertation submitted towards the partial fulfillment of
the requirement for the award of degree of

Master of Technology
in
Microwave and Optical Communication Engineering

Submitted by

Sachin Kakkar
2K13/MOC/10

Under the supervision of

Prof. S.C. Sharma
(HOD, Applied Physics)

Department of Electronics & Communication Engineering and
Department of Applied Physics

Delhi Technological University
(Formerly Delhi College of Engineering)
Delhi-110042
JUNE 2015

DELHI TECHNOLOGICAL UNIVERSITY

Established by Govt. Of Delhi vide Act 6 of 2009

(Formerly Delhi College of Engineering)

SHAHBAD DAULATPUR, BAWANA ROAD, DELHI-110042

CERTIFICATE

This is to certify that work which is being presented in the dissertation entitled **Role of Helical Wiggler on THz Radiation Generation from Free Electron Laser** is the authentic work of **Sachin Kakkar** under my guidance and supervision in the partial fulfillment of requirement towards the degree of **Master of Technology in Microwave and Optical Communication Engineering**, jointly run by Department of Electronics & Communication Engineering and Department of Applied Physics in Delhi Technological University during the year 2013-2015.

As per the candidate declaration this work has not been submitted elsewhere for the award of any other degree.

Prof. S. C. Sharma

Supervisor

H.O.D., Applied Physics

Delhi Technological University

Delhi-110042

DECLARATION

I hereby declare that all the information in this document has been obtained and presented in accordance with academic rules and ethical conduct. This report is my own, unaided work. I have fully cited and referenced all material and results that are not original to this work. It is being submitted for the degree of Master of Technology in Microwave & Optical communication engineering at the Delhi Technological University. It has not been submitted before for any degree or examination in any other university.

Signature :

Name : Sachin Kakkar

ACKNOWLEDGEMENT

I take this opportunity as a privilege to thank all individuals without whose support and guidance I could not have completed my project successfully in this stipulated period of time.

First and foremost I would like to express my deepest gratitude to my supervisor **Prof. S.C. Sharma**, HOD, Applied Physics, for his invaluable support, guidance, motivation and encouragement throughout the period this work was carried out.

I am deeply grateful to **Prof. Prem R. Chadha,** H.O.D. (Deptt. Of E.C.E), **Dr. Ajeet Kumar and Dr. Priyanka Jain** (Branch coordinator, MOC) for their support and encouragement in carrying out this project.

I also wish to express my heart full thanks to the classmates as well as staff at Department of Applied Physics and Electronics & Communication of Delhi Technological University for their goodwill and support that helped me a lot in successful completion of this project.

Finally, I want to thank my parents, sister and friends for always believing in my abilities and for always showering their invaluable love and support.

Sachin Kakkar
M. Tech. (MOC)
2K13/MOC/10

ABSTRACT

Terahertz (THz, or be called T-ray) wave refers to the electromagnetic wave with the frequency between 0.1 THz (1THz=1000GHz) and 10 THz or wavelength from 30 μm to 3000 μm. In the frequency domain, this region of electromagnetic wave is located between microwave and infrared wave. Different from the great successes in the microwave and infrared light wave, the applications of THz wave are much less investigated in the past few decades. Recently, it has recently been demonstrated that THz wave exhibits several unique features in terms of applications. For example, THz wave can easily penetrate fabrics and plastics, but it will be reflected by metallic materials. Thus, THz wave has a promising application in security screening. In order to realize the applications of THz wave, the compact, efficient, and high power THz sources have become a critical element of researches in THz wave.

In this dissertation I have developed the formalism for tunable coherent terahertz radiation generation from a relativistic electron beam, modulated by two laser beams, as it passes through a helical wiggler. The lasers exert a ponderomotive force on beam electrons, and modulate their velocity. In the drift space, velocity modulation translates into density modulation. As the beam bunches pass through the wiggler, they acquire a transverse velocity, constituting a transverse current that acts as an antenna to produce coherent THz radiation.

.

TABLE OF CONTENTS

LIST OF FIGURES

LIST OF TABLES

LIST OF SYMBOLS

$\vec{E}$	Electric Field Intensity
$\vec{B}$	Magnetic Flux Density
d	Modulator Length
L	Drift Space Length
Lw	Wiggler Length
Lb	Electron Bunch Length
v_b	Beam Velocity
c	Speed of Light
k	Wave Number
ω	Frequency
n_b	Electron Beam Density
J_1	First Order Bessel Function
m_e	Mass of Electron
ε_0	Permittivity in free space
μ_0	Permeability in free space
$\vec{F}_p$	Ponderomotive Force
r_b	Electron Bunch Radius
γ_0	Relativistic gamma factor
$\vec{P}_{av}$	Average poynting vector

Chapter 1

Introduction to THz Wave

1.1 Introduction

Terahertz (THz, or be called T-ray) wave refers to the electromagnetic radiations with the frequency ranges from 0.1 THz to 10 THz or wavelength from 30 μm to 3000 μm [1]. This region of radiations is found between microwave and infrared light. Recently, this range have been extended to 40-50THz. Different from the huge application successes for microwave and infrared light, the applications in the THz region are much less considered in the past several decades. However, researchers have not neglected this region and the intense researches related to THz wave started at the beginning of 1990s. Now, two decades has passed, many applications of THz wave have been demonstrated, showing a lot of advantages and unique features that cannot be found in the region of microwave or infrared light. The researches of THz wave are still on-going and many more applications of THz wave will emerge in the near future.

Fig. 1 displays the so-called THz gap in frequency domain. Sources in this region have found many applications, such as THz spectroscopy for studies of carrier dynamics and intermolecular dynamics in liquids [2]. In terahertz spectroscopy, we use photons with energies of about 1 MeV. This energy scale is important for learning about many important aspects of condensed matter physics. At the same time, this power is not strong enough to harm the organic structure, so it is a promising replacement of X ray in medical imaging

Another key feature of THz spectroscopy is that instead of measuring the intensity of the THz pulse, we instead measure the electric field. This means that we have access to information not only about the amplitude change but also the phase change of the electric field as the pulse passes through the medium. It means that we can obtain both the real and imaginary components of the index of refraction. This information usually reflects the intrinsic structure of a crystal.

According to the THz range in electromagnetic spectrum, it can be generated from both the optical and the microwave sides. There are techniques of two categories developed for the generation of THz pulses. One of them includes free electron lasers [3], photoconductive

switching [4] and dipolar antennas. They are sometimes called resonant **optical rectification** since the THz emission results from the polarization change that follows the transport of excited carriers in an applied or surface electric field. In the far-field, the electric field is proportional to the time derivative of the surface current. The bandwidth of the generated pulse is usually limited to a few THz.

Another group of methods, is the non-resonant optical rectification based on nonlinear dielectric crystals. Already in the 1970s, it was shown [5] that picosecond pulses could be rectified in LiNbO3 to produce pulses in the far infrared. In the last few years, it was discovered that optical rectification could be a very efficient method for THz wave generation [6].

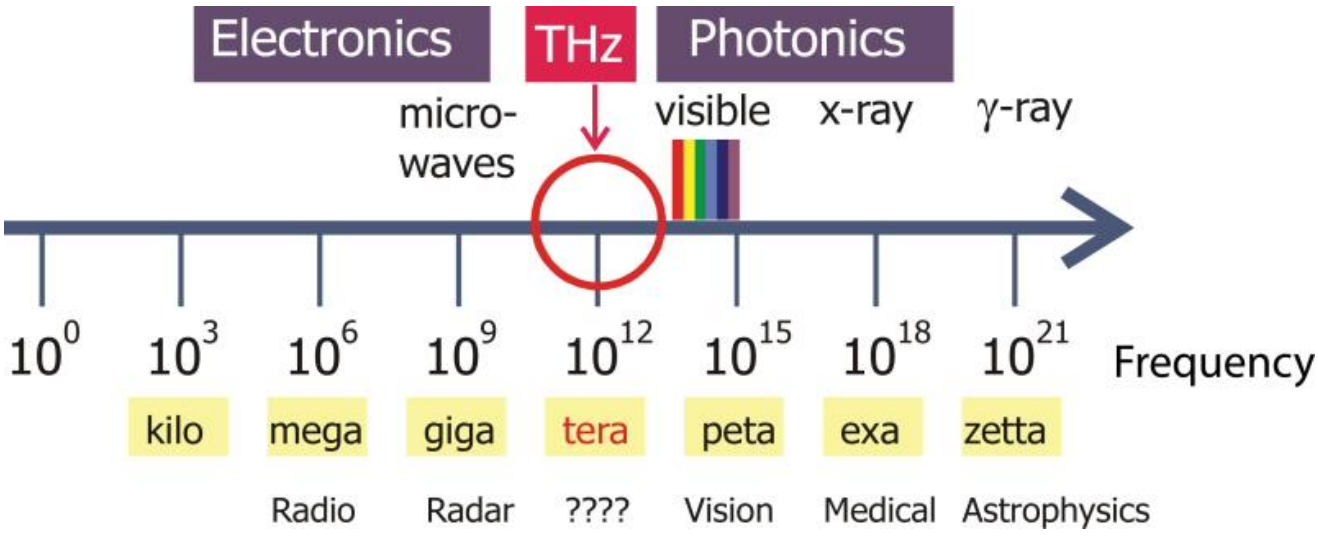

Fig.1.1 Schematic of the electromagnetic spectrum showing that THz wave lies between electronics and photonics.

1.2 Characteristics and Application of THz wave

Regardless of whether THz waves are generated by a CW or pulsed system, the main features that make THz wave technology so interesting can be summarized as follows:

‣ **Fingerprint-** The rotational and vibrational modes of many molecules, especially organic ones, are distributed across the THz band. These modes can be observed as absorption peaks

in the THz spectra. The specific location and amplitude of these absorption peaks can be used to identify the molecules.

‣ **Transparency-** Many dry and non-metallic materials, such as plastic, paper, cardboard, and textiles are transparent to THz waves. This property allows THz waves inspecting samples that are under cover or inside non-optically transparent containers. Microwaves have this see-through capability as well but their larger wavelength compared to THz waves does not allow achieving high resolution images. Infrared can provide much better resolution than THz but infrared waves cannot see through covers.

‣ **Resolution.** Because the wavelength of THz waves is in the range of mm to tens of microns, THz images of macroscopic objects provide lot of details and localized data. This high resolution is a benefit compared to microwaves.

‣ **Safety.** THz photons are non-ionizing and, therefore, do not represent a health hazards for living tissue or humans as X-rays do.

1.2.1 Advantages

(1) THz wave can penetrate fabrics and plastics

(2) THz wave is non-ionizing and may not damage tissue. Thus, THz wave is safer than X-Ray.

(3) Many materials have unique spectral "fingerprints" in the THz wave region.

(4) THz wave has faster frequency than microwaves which means that it can be used in higher-speed communications.

(5) Different from the optical region, it is possible to obtain the phase information of the THz electromagnetic radiation.

1.2.2 Disadvantages

THz-wave imaging has several inherent limitations:

(1) It is not able to penetrate the metal. Metal surface is almost 100 percent reflection index of the THz radiation, THz wave therefore is not able to detect metal objects container.

(2) Water has a strong absorption on the THz wave.

Thus, THz wave cannot propagate very far in atmosphere so that its applications in communication would become very difficult. Besides, the penetration depth of THz wave in tissue is also not very deep (e.g. 4 mm in skin).

1.2.3 Application

In the past two decades, many different applications of THz wave have been developed. Some of these applications will greatly change people's life or even bring some evolutions in different fields. Some of the fields include astrophysics, plasma physics and engineering, materials science and engineering, biomedical engineering, environmental science and engineering, spectroscopy and imaging technology, information science and technology, etc.

(1)Biomedicine

Since many biological macromolecules and DNA molecular rotation and vibration locate in the THz band level generally, the organisms has a unique response to THz wave; therefore, THz radiation can be used for disease diagnosis, organisms detection and imaging, as shown in Fig. 2.

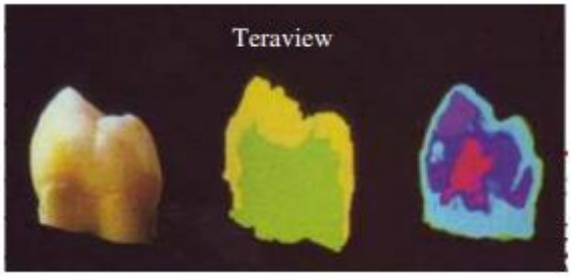

Fig. 1.2 THz tomography of human teeth [18]

Computer-aided tomography technology is the three-dimensional imaging technique, which is developed and applied in the field of X-ray at first. THz wave can also be applied to computer assisted tomography. X-ray tomographic imaging of objects can only reflect the distribution of absorption rate, while the THz tomography record the time waveform information of entire THz pulse. Therefore, according to different requirements can select a different physical detection, such as the electric field strength, peak time and even the spectral characteristics of the material. THz tomography can get not only the absorption rate distribution of objects, but also can get the three-dimensional distribution of the refractive index of objects and materials.

(2) Safety Monitoring and Quality Control

THz radiation can also be used for detecting pollutants, biological and chemical detection, and therefore can be used to monitor the process of food preservation and food processing. The characteristics of THz wave, penetrating objects and security, can be used for non-

contact, non-injury to detect specific substances, such as hidden explosives, drugs, weapons, etc. [19] (as shown in Fig. 3). As a result of the strong capacity of penetration and low energy of THz electromagnetic waves (completely harmless to humans), THz imaging can completely replace the X-ray examination, CT scan, and be used in the material non-destructive monitoring and vital security sector and chemical and biological weapons inspection.

Fig. 1.3: Detection of hidden metal weapons by THz wave.

(3) Non-destructive Testing

The safety and penetrable properties of THz wave can be used for non-destructive testing of building. The penetrability of THz wave can be measured from THz time-domain spectroscopy. Foam is the materials used Space shuttle commonly; the crash of the US space shuttle in 2003, "Columbia" is caused by the degumming of foam isolation in external fuel tank layer. Foam has very low absorption and refractive index on the THz wave, so THz waves can penetrate a few inches thick foam, and to detect the buried defects. THz imaging has been selected as the one of four type of future technology of NASA to detect the defects in space shuttle (the other three technologies for X-ray imaging, ultrasound imaging and laser imaging)

(4) Short Distance Wireless Communications and Networking

THz band has high frequency, wide bandwidth and more channel than the microwave, which is suitable for in local area networks and broadband mobile communications. 10 Gbps wireless transmission speeds can be obtained by THz communication, which is a few hundred or even thousands of times faster than current Ultra-Wideband technology, and is the future

hope for large-capacity multimedia wireless communications. Some experts predict that in the near future THz wireless network will replace the wireless LAN or Bluetooth technology, become the major short-range wireless communications technology.

(5) Secure Communication

In outer space, the transmission of THz is lossless, so we can achieve long-range space communications with very little power. At the same time, compared with the current space optical communication, THz wave has wider beam width, so it is easier to pointing in the long-distance space communication. And antenna system can achieve small and flat, and is particularly suited for secure communications between the stars and satellites.

Some other Applications

(1) Cosmology and radio astronomy
(2) Atmospheric remote sensing
(3) Plasma fusion diagnostics and heating
(4) Radar modeling
(5) Material measurement
(6) Local area networks and narrowing
(7) Anti-collision radar for cars
(8) Windshear detection for aircraft
(9) Radar ground movement for aircraft
(10) Medical sensing
(11) Airport security inspection

1.3 Terahertz Wave Sources

As mentioned in the introduction, the intense researches related to terahertz wave can date back to early 1990s. Now, almost twenty five years has passed, most of the applications and explorations are still limited within laboratories and carried out only on optical table. It is easy for us to associate THz wave with the invention of laser in 1960. Twenty years after that, the researches and applications blossomed at an extremely fast speed. But why is it not so in terahertz domain? One of the most important reasons seems quite obvious. Although different methods have been explored, we are still in short of efficient, compact, powerful terahertz sources that could operate at room temperature.

It is important to list the present THz wave sources and point out their shortcomings and limitations.

1.3.1 Broadband Terahertz Sources

Blackbody Radiation

High-temperature blackbody emitters can provide incoherent radiation in the THz range. This kind of sources have already been used in the THz Fourier transform infrared (FTIR) spectrometer. The THz FTIR spectrometer has also been used to fingerprint many different of materials, like DNA's and proteins [7]. However, it is still difficult to create useful terahertz power levels with a blackbody source, because the generated THz power can only reach about 1nW per wave number

Photoconduction

Terahertz wave photoconduction emitter is based on ultrafast laser pulses. Free carriers-electrons and holes are generated in the photoconductor which is excited by the ultrafast pulses. The static bias fields then accelerate the free carriers and generate a transient photocurrent, resulting in the fast and time changing current which radiates electromagnetic waves in the THz domain. The THz wave bandwidth is about 4 THz and the highest output power is about tens of μW.

However, the photoconductor has the drawback of breakdown voltage which greatly limits the output power. [1][8][9]

Optical Rectification

This kind of the method also needs the excitation of ultrafast laser. Optical rectification is a nonlinear optical process which consists in the generation of a DC polarization in a nonlinear optical medium pumped by the ultrafast laser pulses. The output THz wave power is related to the second-order nonlinear coefficient of materials and does not have the upper limit voltage characteristics in photoconduction. The output power will then be limited by the optical damage threshold of the materials and the problem of optical phase-matching. [8]

Air Plasma

This is demonstrated in recent years and will also need very intense ultrafast laser pulses. The advantage is that none special medium is used in the process of generation and air is actually the emitter of the terahertz wave. The ionized plasma is the main mechanism of the efficient THz wave generation and it is actually a third-order nonlinear optical process. [10]

1.3.2 Narrowband Terahertz Sources

Difference Frequency Generation

Difference frequency generation (DFG) is one of the second-order nonlinear optical processes, in which new photon at $\omega 3$ is generated when exciting the nonlinear optical medium both at $\omega 1$ and $\omega 2$ simultaneously ($\omega 3 = \omega 1 - \omega 2$). The generation of THz wave based on DFG is not a new topic. The experimental demonstration is as early as in the 1970s. However, because of the lack of application in the THz domain at that time, this technique was not further investigated. In recent years, THz wave generation from DFG attracts increasing attentions due to the lack of efficient and powerful THz sources. The efficient, tunable, and coherent THz source can cover as wide as 0.185~5.27 THz [11].

Up conversion from RF Source

This method is based on the microwave technology and is often obtained by cascading a chain of planar GaAs Schottky-diode multipliers. To achieve THz with higher frequency, the frequency has to be doubled or even tripled with a lot of output power sacrificed each time as this process is applied. These kinds of THz sources are achievable under 1 THz and are very difficult to reach higher frequency.

*CO*2 **THz lasers**

*CO*2 gas THz lasers can give an average output power as high as 100 mW at THz region. This kind of laser use the high power *CO*2 gas lasers as the pump source and excites gas molecules emission-line (e.g. methanol). Although the high output power is very impressive, the wavelength cannot be tuned continuously and can only cover some discrete emission frequencies. Besides, the whole dimension of the laser is very big and can only be used on optical table in laboratory.

Free-electron Laser

Different from the gas, solid-state, diode lasers, the gain medium in the free-electron laser is relativistic electron beam that moves freely through a periodic magnetic structure. It has the widest tunable wavelength range, which covers from the microwaves to X-rays. The THz domain is included in its tunable range. However, because of its huge dimension and operating complexity, it is only available in some large universities and research institutes.

Quantum Cascade Lasers

Quantum-cascade laser (QCL) is based on intersubband transitions of electrons inside a quantum-well structure. Unlike other semiconductor light sources, the emitted wavelength is not determined by the band gap of the used material but on the thickness of the constituent layers [12,13]. QCL obtained complete victory in generating mid-infrared radiation and also is considered to be one of the best candidates for compact THz source. Lots of researches on quantum-cascade terahertz lasers have been reported [14,15,16,17]. The only intrinsic drawback is that quantum-cascade terahertz laser cannot operate at room-temperature.

Chapter 2

Free Electron Laser (FEL)

2.1 Free-electron laser (FEL)

A free electron laser (FEL) is a high power microwave devices in which a relativistic electron beam (REB) propagating through a periodic magnetic field is used to amplify or generate coherent electromagnetic radiation.

A free-electron laser (FEL), is a high power microwave device in which very-high-speed electrons move freely through a magnetic structure,[20] that's why the term free electron as the lasing medium[21]. The free-electron laser has the widest frequency range of any laser type, and can be widely tunable[22], currently ranging in wavelength from microwaves, through terahertz radiation and infrared, to the visible spectrum, ultraviolet, and X-ray[23].

The term free-electron laser was given by John Madey in 1976 at Stanford University [24]. The work emanates from research done by Hans Motz and his coworkers, who built an undulator at Stanford in 1953[24,25], using the wiggler magnetic configuration which is the heart of a free electron laser. Madey used a 43-MeV electron beam [26] and 5 m long wiggler to amplify a signal.

To create an FEL, a beam of electrons is accelerated about the speed of light. The beam passes through a wiggler, a side to side magnetic field produced by a periodic arrangement of magnets with alternating poles across the beam path. The direction of the beam is called the longitudinal direction, while the direction across the beam path is called transverse. This array of magnets is called a wiggler, because it forces the electrons in the beam to wiggle transversely along a sinusoidal path about the axis of the wiggler.

The transverse acceleration of the electrons across this path results in the release of photons (synchrotron radiation), which are monochromatic but still incoherent, because the electromagnetic waves from randomly distributed electrons interfere constructively and destructively in time, and the resulting radiation power scales linearly with the number of electrons. If an external laser is provided or if the synchrotron radiation becomes sufficiently

strong, the transverse electric field of the radiation beam interacts with the transverse electron current created by the sinusoidal wiggling motion, causing some electrons to gain and others to lose energy to the optical field via the ponderomotive force.

This energy modulation evolves into electron density (current) modulations with a period of one optical wavelength. The electrons are thus clumped, called *microbunches*, separated by one optical wavelength along the axis. Whereas conventional wiggler would cause the electrons to radiate independently, the radiation emitted by the bunched electrons are in phase, and the fields add together coherently.

The FEL radiation intensity grows, causing additional microbunching of the electrons, which continue to radiate in phase with each other [27]. This process continues until the electrons are completely microbunched and the radiation reaches a saturated power several orders of magnitude higher than that of the wiggler radiation.

The wavelength of the radiation emitted can be tuned by varying the wiggler wavelength or adjusting the energy of the electron beam.

2.2 Ponderomotive force

A ponderomotive force is a nonlinear force in which a charged particle experiences an oscillating electromagnetic field in inhomogeneous medium.

The ponderomotive force $\vec{F}_p$ is expressed by

$$\vec{F}_p = \frac{-e}{2}\left(\vec{v} \times \vec{B}\right) ,$$

where *e* is the electronic charge of the particle, *B* is the magnetic flux density (low enough that magnetic field exerts very little force) , v is the oscillation velocity of electron beam of frequency ω.

This equation means that a charged particle in an inhomogeneous oscillating field oscillates at the frequency of ω as well as drifts toward the weak field area.

The mechanism of the ponderomotive force is that the motion of the charge in an oscillating electric field. In homogeneous field the charge proceeds to its initial position after one cycle

of oscillation while in inhomogeneous field the force experienced by the charge during the half-cycle it spend in the area with higher field amplitude points towards the weak field amplitude. The force exerted during the half-cycle spent in the area with a higher field amplitude is larger than the field force exerted during the half-cycle spent in the area with a weak amplitude. Thus, averaged over a full cycle there is a net force that drives the charge toward the weak field area.

2.3 Optical modulator

An optical modulator is a device used to modulate a beam of light. The beam carried over free space, or propagated through an optical fiber.

Depending on the parameter of a light beam modulators may be categorized into-

(1) Amplitude modulator.

(2) Phase modulator.

(3) Polarization modulator.

The easiest method to obtain modulation of intensity of a light beam, is to modulate the current driving the light source that is a laser diode. This scheme of modulation is called direct modulation as different to the external modulation perform by a light modulator. For laser diode narrow line width is required due to which a high bandwidth chirping effect when applying and removing the current to the laser so direct modulation is avoided.

Classification of optical modulators

According to the properties of the material which modulate the light beam, modulators are divided into two groups:-

(1) **Refractive modulators**-In this modulation refractive index of the material is changed. Refractive modulator use of an electro-optic effect. In Refractive modulator change of the refractive index and permittivity is due to pockels effect, kerr effect, and electron-gyration

(2) **Absorptive modulators** – In this modulators absorption coefficient of the material is changed. The absorption coefficient of the material can be manipulated by the Quantum-

confined excitonic absorption, Stark effect, Franz-Keldysh effect, changes of Fermi level, or changes of free carrier concentration. If several such effects come out together, the modulator is called an electro-absorptive modulator.

2.4 Helical Wiggler

A helical wiggler is an insertion device in a synchrotron. Helical wiggler is a series of magnet designed to periodically (shown in Fig) deflect a beam of charged particles inside a storage ring of a synchrotron. These deflections create a change in acceleration that will provide turn produces emission of broad synchrotron radiation tangent to the curve, but the intensity is higher due to the contribution of many magnetic dipoles in the wiggler. Furthermore, as the wavelength λ_w is decreased this means the frequency f has increased. This increase of frequency is directly proportional to energy; hence, the wiggler creates a wavelength of light with a larger energy.

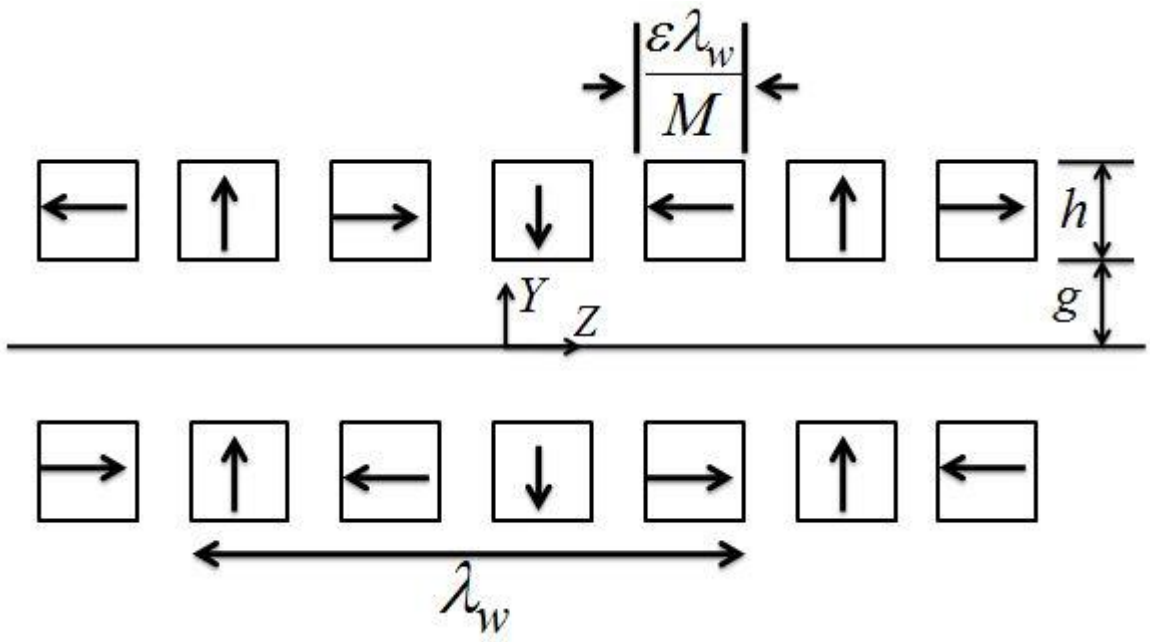

Fig 2.1 Vertical cross section view of wiggler / undulator with four blocks per period.

where h is the height of the blocks, g is the full gap and M' is the number of blocks per period in each half of the device. The value of M=4 in the above fig. Device is effective when the width of the blocks in the X Direction is much greater than the gap width g.

2.5 Drift Space-

Drift or bunching space is a region where slow electron are speeded up or accelerated to overtake the fast moving electron and fast moving electron are deaccelerated to catch up the slow moving electron that turns into the density modulation of the beam electron.

Chapter 3

Mathematical Analysis

3.1 Overview

In this chapter, we derive the mathematical analysis for laser beat modulation of an electron beam and THz generation from the density bunched electron beam in a helical wiggler. The process of THz generation is as follows: Two lasers with a frequency difference $\omega_{01} - \omega_{02}$ in the THz range apply a ponderomotive force on the beam electrons modulating their velocity. In the drift space, velocity modulation turns into density modulation. The electrons that arrive the modulator at a time when the electric field is parallel to v_b (where v_b is the initial electron beam velocity), get retarded and emerge from the modulator with reduced velocity. The electrons that arrive half wave period later when the electric field is anti-parallel to v_b get accelerated and emerge with larger velocity. In the drift space, fast moving electrons catch with slow moving electrons and cause density bunching. As the beam bunches pass through the wiggler, they acquire a transverse velocity, constituting a transverse current producing coherent THz radiation.

3.2 Modulation

By following the analysis of Kumar and Tripathi [28]

Consider two laser beams of frequencies ω_{01} and ω_{02} propagating in a modulator with electric field,

$$\vec{E}_{01} = A_1 e^{-i(\omega_{01}t - k_{01}z)}\hat{x}$$

$$\vec{E}_{02} = A_2 e^{-i(\omega_{02}t - k_{02}z)}\hat{x}$$

We will find out the magnetic field associated with this field by using Maxwell Equations

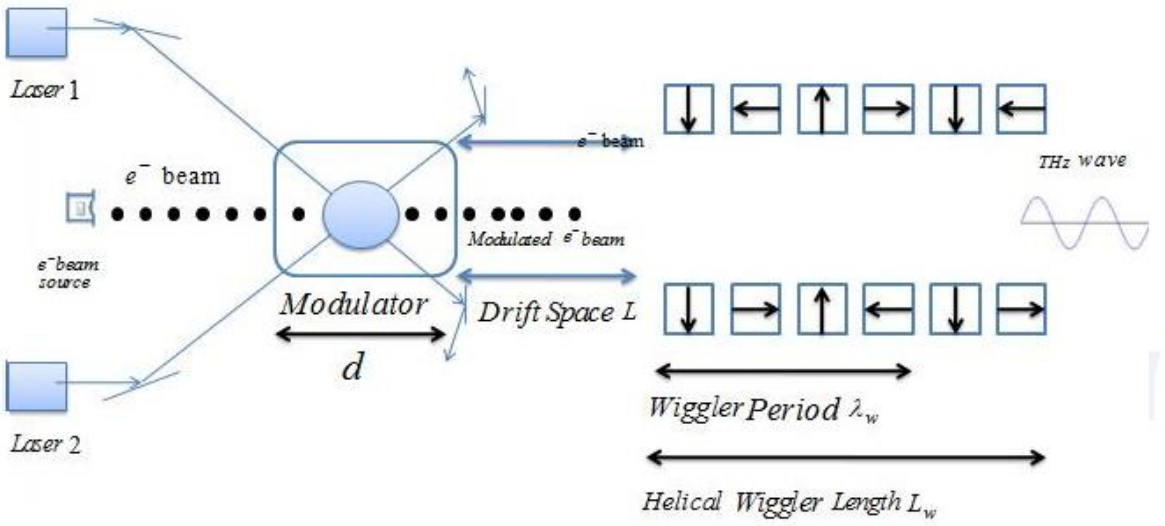

Fig 3.1 Schematic diagram of THz radiation generation by electron bunch coupling to helical Wiggler after following Ref. [28]

$$\nabla \times \vec{E} = -\frac{\partial \vec{B}}{\partial t}$$

$$\nabla \times \vec{E}_{01} = -\frac{\partial \vec{B}_{01}}{\partial t} \qquad \nabla \times \vec{E}_{02} = -\frac{\partial \vec{B}_{02}}{\partial t}$$

Replace $\frac{\partial}{\partial t} \to i\omega$ and by solving $\nabla \times \vec{E}_{01} = -\frac{\partial \vec{B}_{01}}{\partial t}$

$$\left(\frac{\partial}{\partial x}\hat{x} + \frac{\partial}{\partial y}\hat{y} + \frac{\partial}{\partial z}\hat{z}\right) \times \left(A_1 e^{-i(\omega_{01}t - k_{01}z)}\hat{x}\right) = \frac{\partial \vec{B}_{01}}{\partial t}$$

$$A_1 e^{-i(\omega_{01}t - k_{01}z)}\left(ik_1\right)\hat{y} = -i\omega_{01}\vec{B}_{01}$$

$$\vec{B}_{01} = -\frac{A_1 k_{01}}{\omega_{01}} e^{-i(\omega_{01}t - k_{01}z)}\hat{y} \qquad (1)$$

Similarly, we get

$$\vec{B}_{02} = -\frac{A_2 k_{02}}{\omega_{02}} e^{-i(\omega_{02}t - k_{02}z)} \hat{y} \tag{2}$$

A relativistic electron beam of density n_b, velocity $v_b \hat{z}$, and cross-section A_b passes through the modulator of width d. The lasers impart an oscillatory velocity to the beam electron

$$\vec{v}_1 = \frac{e\vec{E}_{01}}{m_e i\omega_{01}\gamma_0} \quad , \tag{3}$$

$$\vec{v}_2 = \frac{e\vec{E}_{02}}{m_e i\omega_{02}\gamma_0} \quad , \tag{4}$$

where -e and m_e are the charge and rest mass of electrons and $\gamma_0 = \left(1 - \frac{{v_{0b}}^2}{c^2}\right)^{-1/2}$ is the relativistic gamma factor.

Lasers also apply a terahertz ponderomotive force on them,

$$\vec{F} = -\frac{e}{2}\left(\vec{v}_1 \times \vec{B}_{02}^{*} + \vec{v}_2^{*} \times \vec{B}_{01}\right) \tag{5}$$

First we solve –

$\vec{v}_1 \times \vec{B}_{02}^{*}$

$$\vec{v}_1 \times \vec{B}_{02}^{*} = \frac{eA_1 e^{-i(\omega_{01}t - k_{01}z)}\hat{x}}{m_e i\omega_{01}\gamma_0} \times \left(-\frac{A_2^{*} k_{02}}{\omega_{02}} e^{i(\omega_{02}t - k_{02}z)}\right)\hat{y} \tag{6}$$

$$= -\frac{eA_1 {A_2}^{*} k_2}{m_e i\omega_{01}\omega_{02}\gamma_0} e^{-i[(\omega_{01}-\omega_{02})t - (k_{01}-k_{02})z]}\hat{z}$$

$$\vec{v}_1 \times \vec{B}_{02}^{*} = -\frac{eA_1 {A_2}^{*} k_2}{m_e i\omega_{01}\omega_{02}\gamma_0} e^{-i(\omega t - kz)}\hat{z}$$

where $\omega_{01} - \omega_{02} = \omega$ and $\vec{k}_{01} - \vec{k}_{02} = \vec{k}$

Similarly we will find $\vec{v}_2^* \times \vec{B}_{01}$

$$\vec{v}_2^* \times \vec{B}_{01} = \frac{eA_1A_2^*k_1}{m_e i\omega_{01}\omega_{02}\gamma_0} e^{-i(\omega t - kz)}\hat{z} \tag{7}$$

Substituting values of (6) and (7) in Equation (5), we get

$$\vec{F} = -\frac{e}{2}\left(-\frac{eA_1A_2^*k_2}{m_e i\omega_{01}\omega_{02}\gamma_0} e^{-i(\omega t - kz)} + \frac{eA_1A_2^*k_2}{m_e i\omega_{01}\omega_{02}\gamma_0} e^{-i(\omega t - kz)} \right)\hat{z}$$

$$= -\frac{e^2 A_1A_2^*}{2m_e i\omega_{01}\omega_{02}\gamma_0}\left(k_{01} - k_{02}\right)e^{-i(\omega t - kz)}\hat{z}$$

$$= -\frac{e^2 A_1A_2^*k}{2m_e i\omega_{01}\omega_{02}\gamma_0} e^{-i(\omega t - kz)}\hat{z}$$

$$\vec{F} = \vec{F}_0 e^{-i(\omega t - kz)}\hat{z}$$

where

$$\vec{F}_0 = -\frac{e^2 A_1A_2^*k}{2m_e i\omega_{01}\omega_{02}\gamma_0} \tag{8}$$

As a practical scheme of modulation, we consider two laser beams of spot diameter $2r_0$ each, colliding with each other at an angle θ_d. Then, the length of the overlap region is

$$d = \frac{2r_0}{\sin\left(\frac{\theta_d}{2}\right)} \approx \frac{2r_0}{\frac{\theta_d}{2}} = \frac{4r_0}{\theta_d}$$

In this case, ponderomotive force z component is still F_0 with k replaced by $k\cos\theta_d$. For $\theta_d \ll 1;\ k\cos\theta_d \approx k$ and above expression for ponderomotive force remains same.

Let t_0 be the time at which an electron reaches the modulator (z=0), t_1 at which it leaves the modulator at z=d, and t_2 at which it reaches the wiggler placed after a drift space of length L. Inside the modulator motion under the ponderomotive force is governed by the relativistic equation of motion

$$\frac{\partial}{\partial t}\left(\gamma\vec{v}\right) = \frac{\vec{F}_p}{m_e}\ , \tag{9}$$

where $\vec{v} = v_b \hat{z} + v_{b\omega} \hat{z}$ and $\gamma = \gamma_0 + {\gamma_0}^3 \frac{v_b v_{b\omega}}{c^2}$

$$\gamma \vec{v} = \left(\gamma_0 + {\gamma_0}^3 \frac{v_b v_{b\omega}}{c^2} \right) \left(v_b + v_{b\omega} \right) \hat{z}$$

$$= \left(\gamma_0 v_b + \gamma_0 v_{b\omega} + {\gamma_0}^3 \frac{{v_b}^2 v_{b\omega}}{c^2} + {\gamma_0}^3 \frac{v_b {v_{b\omega}}^2}{c^2} \right) \hat{z}$$

In order to linearize the equation we make the approximation, then

$$\gamma \vec{v} \cong \left({\gamma_0}^3 v_{b\omega} \right)$$

From (9), $\frac{d}{dt}\left({\gamma_0}^3 \vec{v} \right) = \frac{\vec{F}}{m_e}$ (10)

In the exponent, we take $z = v_b \left(t - t_0 \right)$ and integrate Eq.(10) from t_0 to $t_1 = t_0 + \frac{d}{v_b}$,we get

$$\int_0^{v_{b\omega_m}} d\left({\gamma_0}^3 v_{b\omega} \right) = \int_{t_0}^{t_0 + d/v_b} \frac{\vec{F}_0}{m_e} e^{-i\left[\omega t - v_b (t - t_0) k \right]} dt$$

$$ {\gamma_0}^3 v_{b\omega} = \frac{\vec{F}_0}{m_e} \left[\frac{e^{-i\left[\omega t - v_b (\mathrm{t} - \mathrm{t}_0) \mathrm{k} \right]}}{-i(\omega - v_b \, \mathrm{k})} \right]_{t_0}^{t_0 + d/v_b}$$

$$ {\gamma_0}^3 v_{b\omega} = \frac{\vec{F}_0}{-i m_e \left(\omega - v_b k \right)} \left[e^{-i\left(\omega t_0 + \left(\frac{\omega - v_b k}{v_b} \right) d \right)} - e^{-i(\omega t_0)} \right]$$

$$ {\gamma_0}^3 v_{b\omega} = \frac{\vec{F}_0}{-i m_e \left(\omega - v_b k \right)} e^{-i\left(\omega t_0 + \left(\frac{\omega - v_b k}{2 v_b} \right) d \right)} \left[e^{-i\left(\frac{\omega - v_b k}{2 v_b} \right)} - e^{i\left(\frac{\omega - v_b k}{2 v_b} \right)} \right]$$

$$v_{b\omega} = \frac{-\vec{F}_0}{m_e v_b {\gamma_0}^3} \frac{\sin \theta_g}{\theta_g} e^{-i(\omega t_0 + \theta_g)} \hat{z}$$

where $\theta_g = \left(\frac{\omega - v_b k}{2 v_b} \right) d$ is the modulator phase angle.

Substituting value of $\vec{F}_0$ from Eq. (8) in $v_{b\omega_m}$

$$v_{b\omega} = \frac{-e^2 k A_1 A_2^{*} d}{2i\omega_{01}\omega_{02} m_e^2 v_b \gamma_0^{\,4}} \frac{\sin\theta_g}{\theta_g} e^{-i(\omega t_0 + \theta_g)} \hat{z}$$

$$v_{b\omega} = \frac{ie^2 k A_1 A_2^{*} d}{2\omega_{01}\omega_{02} m_e^2 v_b \gamma_0^{\,4}} \frac{\sin\theta_g}{\theta_g} \left[\cos(\omega t_0 + \theta_g) - i \sin(\omega t_0 + \theta_g) \right] \hat{z} \tag{11}$$

By considering real terms

$$v_{b\omega} = \frac{-e^2 k A_1 A_2^{*} d}{2\omega_{01}\omega_{02} m_e^2 v_b \gamma_0^{\,4}} \frac{\sin\theta_g}{\theta_g} \sin(\omega t_0 + \theta_g) \hat{z}$$

$$v_{b\omega} = -\psi v_b \sin(\omega t_0 + \theta_g)\, \hat{z}$$

$$\psi = \frac{k d c^2}{2 v_b^2 \gamma_0^4} \frac{e A_1}{m_e \omega_{01} c} \frac{e A_2^{*}}{m_e \omega_{02} c} \frac{\sin\theta_g}{\theta_g} \tag{12}$$

In the drift space, the fast moving electrons catch up with the slow moving ones that had left the modulator half wave period earlier, leading to density bunching of electrons. The time of arrival of the electron bunch at the entry point z (z=d+L) to the wiggler is $t_{2=}t_0 + \left(d \big/ v_b \right) + \left(L(1 + \psi \sin(\omega t_0 + \theta_g)) / v_b \right)$. Let the beam current at the wiggler be I_2. Then, the charge passing through any cross-section in time dt_2 at the wiggler is $I_2 dt_2$. This must be equal to the charge entering the modulator between t_0 and $t_0 + dt_0$, i.e., $I_2 = I_0 \big/ \left(dt_2 / dt_0 \right)$. I_2 is a periodic function of time. We may expand it in Fourier series,

$$I_2(t_2) = a_0 + a_1 \cos\omega t_2 + a_2 \cos\omega t_2 + \ldots\ldots + b_1 \sin\omega t_2 + b_2 \sin\omega t_2 + \ldots\ldots\ldots\ldots$$

where

$$a_1 = \frac{\omega}{\pi} \int_0^{2\pi/\omega} I_2 dt_2 \cos\omega t_2$$

$$= \frac{\omega}{\pi} \int_0^{2\pi/\omega} I_2 dt_0 \cos\left(\omega t_0 + \frac{\omega(d+L)}{v_b} + \frac{\omega L \psi}{v_b} \sin\left[\omega t_0 + \theta_g \right] \right)$$

$$b_1 = \frac{\omega}{\pi}\int_0^{2\pi/\omega} I_2 dt_2 \sin\omega t_2$$

$$= \frac{\omega}{\pi}\int_0^{2\pi/\omega} I_2 dt_0 \sin\left(\omega t_0 + \frac{\omega(d+L)}{v_b} + \frac{\omega L\psi}{v_b}\sin\left[\omega t_0 + \theta_g\right]\right)$$

If we introduce

$$\phi = \frac{\omega I_0}{\pi}\int_0^{2\pi/\omega} \exp\left(i\omega\left(t_0 + \frac{d+L}{v_b}\right)\right)\times\exp\left(\frac{i\omega L\psi\sin(\omega t_0+\theta_g)}{v_b}\right)dt_0$$

then $a_1 = \mathrm{Re}(\phi)$ and $b_1 = \mathrm{Im}(\phi)$.Employing the Bessel function identity,

$e^{i\alpha\sin\theta} = \sum_{n=-\infty}^{\infty} J_n(\alpha)e^{in\theta}$,we may write,

$$\phi = \frac{\omega I_0}{\pi}\sum_n \int_0^{2\pi/\omega} J_n\left(\omega L\psi / v_b\right)e^{i\left(\omega(d+L)/v_b\right)}e^{i(n+1)\omega t_0}e^{in\theta_g}dt_0$$

Using the orthonormality relation, we find that all terms in ϕ ,other than n= -1 term, vanish, giving

$$\phi = -2I_0 J_1\left(\omega L\psi/v_b\right)e^{i\left(\omega(d+L)/v_b-\theta_g\right)}$$

Hence,

$$a_1 = -2I_0 J_1\left(\omega L\psi/v_b\right)\cos\left((\omega(d+L)/v_b)-\theta_g\right)$$

$$b_1 = -2I_0 J_1\left(\omega L\psi/v_b\right)\sin\left((\omega(d+L)/v_b)-\theta_g\right)$$

The ω frequency component of I_2 is

$$I_2(\omega) = \mathrm{a}_1\cos(\omega\mathrm{t}_2) + \mathrm{b}_1\sin(\omega\mathrm{t}_2)$$

$$= -2\,\mathrm{I}_0\,J_1\left(\omega L\psi/v_b\right)\cos(\omega\mathrm{t}_2-\delta)$$

where $\delta = \frac{\omega(d+L)}{v_b} - \theta_g$, $I_0 = -n_b e v_b A_b$

The beam density modulation at the wiggler can be written as

$$n_{\omega,k} = -\frac{I_2(\omega)}{e v_b A_b} = -2n_b J_1\left(\omega L\psi / v_b\right)\cos(\omega t_2 - \delta) \tag{13}$$

We allow the electron bunch to enter the Helical wiggler magnetic field-

$$\vec{B} = \vec{B}_0(\hat{\rho} - \mathrm{i}\hat{\varphi})\mathrm{e}^{-i(\mathrm{k}_0 z+\varphi)}$$

In this field, electrons acquire an oscillatory velocity which in the beam frame, moving with velocity $\vec{v}_0^{'}$ can be written as

$$\vec{v}_0^{'} = \frac{e\vec{E}_0^{'}}{m_e i\omega_0^{'}} \tag{14}$$

where $\omega_0^{'} = \gamma_0 k_0 v_b$

where prime denotes the Lorentz-transformed quantities in the moving frame

$$\vec{E}_0^{'} = \gamma_0 v_b \hat{z} * \vec{\mathrm{B}}_0(\hat{\rho} - \mathrm{i}\hat{\varphi})\mathrm{e}^{-i(\omega_0^{'}t^{'} - k_0^{'}z^{'}+\varphi)}$$

$$= \gamma_0 v_b \hat{z}\,\vec{\mathrm{B}}_0(\hat{\varphi} + i\hat{\rho})\mathrm{e}^{-i(\omega_0^{'}t^{'} - k_0^{'}z^{'}+\varphi)}$$

$$\vec{E}_0^{'} = -\frac{\gamma_0}{i} v_b\,\vec{\mathrm{B}}_0(\hat{\rho} - \mathrm{i}\hat{\varphi})\mathrm{e}^{-i(\omega_0^{'}t^{'} - k_0^{'}z^{'}+\varphi)} \tag{15}$$

Substitute the value of Eq. (15) in Eq. (14), we get

$$\vec{v}_0^{'} = -\frac{e}{m_e i\omega_0^{'}}\frac{\gamma_0}{i} v_b\,\vec{\mathrm{B}}_0(\hat{\rho} - \mathrm{i}\hat{\varphi})\mathrm{e}^{-i(\omega_0^{'}t^{'} - k_0^{'}z^{'}+\varphi)}$$

$$\vec{v}_0^{'} = \frac{e}{m_e\omega_0^{'}}\gamma_0 v_b\,\vec{\mathrm{B}}_0(\hat{\rho} - \mathrm{i}\hat{\varphi})\mathrm{e}^{-i(\omega_0^{'}t^{'} - k_0^{'}z^{'}+\varphi)} \tag{16}$$

3.3 Power Expression of THz wave

Non Linear current density is given by

$$\vec{J}_{NL} = -n_{\omega,k} e\vec{v}_0^{'}$$

From Eq. (13) and Eq. (16)

$$\vec{J}_{NL} = 2n_b J_1\left(\frac{\omega L\psi}{v_b}\right)e^{-i(\delta-\varphi)}e^{-i\omega t_2} \times e \times \frac{e}{m_e\omega_0^{'}}\gamma_0 v_b\,\vec{\mathrm{B}}_0(\hat{\rho} - \mathrm{i}\hat{\varphi})\mathrm{e}^{-i(\omega_0^{'}t^{'} - k_0^{'}z^{'})}$$

$$\vec{J}_{NL} = 2n_b J_1\left(\frac{\omega L\psi}{v_b}\right) e^{-i(\delta-\varphi)} \frac{e^2}{m_e\omega_0^{'}} \gamma_0 v_b \vec{B}_0(\hat{\rho} - \mathrm{i}\hat{\varphi}) \mathrm{e}^{-i(\omega t_2 + \omega_0^{'} t^{'} - k_0^{'} z^{'})}$$

Put $t_2 = t^{'} - \frac{z^{'}}{v_b}$

$$\vec{J}_{NL} = \frac{2n_b J_1\left(\frac{\omega L\psi}{v_b}\right) e^2 v_b \gamma_0 B_0\left(\hat{\rho} - i\hat{\varphi}\right)}{m_e\omega_0^{'}} e^{-i\left(\omega t^{'} - \frac{\omega z^{'}}{v_b} + \omega_0^{'} t^{'} - k_0^{'} z^{'}\right)} e^{i(\delta-\varphi)}$$

$$\vec{J}_{NL} = \frac{2n_b J_1\left(\frac{\omega L\eta}{v_b}\right) e^2 v_b \gamma_0 B_0\left(\hat{\rho} - i\hat{\varphi}\right)}{m_e\omega_0^{'}} e^{-i\left[\left(\omega+\omega_0^{'}\right)t - \left(\frac{\omega}{v_b} + k_0^{'}\right) z^{'}\right]} e^{i(\delta-\varphi)}$$

Let $\omega_s = \omega + \omega_0^{'}$

$$\vec{J}_{NL} = \frac{2n_b J_1\left(\frac{\omega L\psi}{v_b}\right) e^2 v_b \gamma_0 B_0\left(\hat{\rho} - i\hat{\varphi}\right)}{m_e\omega_0^{'}} e^{-i\left[\omega_s t - \left(\frac{\omega}{v_b} + k_0^{'}\right) z^{'}\right]} e^{i(\delta-\varphi)} \qquad (17)$$

Now Retarded vector potential is given by

$$\vec{A}(\vec{r},t) = \frac{\mu_0}{4\pi}\int \frac{\vec{J}\left(\vec{r}, t - \frac{R}{c}\right)}{R} d^3 r^{'} \quad ,$$

where $R = \left|\vec{r} - \vec{r}^{'}\right| = r - z^{'}\cos\theta$

$$\vec{A}(\vec{r},t) = \frac{\mu_0}{4\pi}\int \frac{\vec{J}\left(\vec{r}, t - \frac{R}{c}\right)}{r} 4\pi r_b^2 dz^{'}$$

$$\vec{A}(\vec{r},t) = \frac{\mu_0 r_b^2}{r}\int \vec{J}\left(\vec{r}, t - \frac{R}{c}\right) dz^{'} \qquad (18)$$

Substituting the value of $\vec{J}$ from Eq. (17) in Eq. (18),we get

$$\vec{A}(\vec{r},t)=\frac{\mu_0 r_b^2}{r}\int\frac{2n_b J_1\left(\frac{\omega L\psi}{v_b}\right)e^2 v_b\gamma_0 B_0\left(\hat{\rho}-i\hat{\varphi}\right)}{m_e\omega_0^{'}}e^{i(\delta-\varphi)}e^{-i\left(\omega_s\left(t-\frac{R}{c}\right)-\left(\frac{\omega}{v_b}+k_0^{'}\right)z^{'}\right)}dz^{'}$$

$$\vec{A}(\vec{r},t)=\frac{\mu_0 r_b^2}{r}\frac{2n_b J_1\left(\frac{\omega L\psi}{v_b}\right)e^2 v_b\gamma_0 B_0\left(\hat{\rho}-i\hat{\varphi}\right)}{m_e\omega_0^{'}}e^{i(\delta-\hat{\varphi})}\int e^{-i\left(\omega_s\left(t-\frac{r-z^{'}\cos\theta}{c}\right)-\left(\frac{\omega}{v_b}+k_0^{'}\right)z^{'}\right)}dz^{'}$$

$$\vec{A}(\vec{r},t)=\frac{\mu_0 r_b^2}{r}\frac{2n_b J_1\left(\frac{\omega L\psi}{v_b}\right)e^2 v_b\gamma_0 B_0\left(\hat{\rho}-i\hat{\varphi}\right)}{m_e\omega_0^{'}}e^{i(\delta-\varphi)}e^{-i\left(\omega_s\left(t-\frac{r}{c}\right)\right)}\int e^{-i\left(\frac{\omega_s\cos\theta}{c}-\frac{\omega}{v_b}-k_0^{'}\right)z^{'}}dz^{'}$$

Let $I=\int_0^{L_b}e^{-i\left(\frac{\omega_s\cos\theta}{c}-\frac{\omega}{v_b}-k_0^{'}\right)z^{'}}dz^{'}$

where L_b is bunch length.

$$I=\frac{e^{i\left(\frac{\omega}{v_b}-\frac{\omega_s\cos\theta}{c}+k_0^{'}\right)L_b}-1}{i\left(\frac{\omega}{v_b}-\frac{\omega_s\cos\theta}{c}+k_0^{'}\right)}$$

$$\vec{A}(\vec{r},t)=\frac{\mu_0 r_b^2}{r}\frac{2n_b J_1\left(\frac{\omega L\psi}{v_b}\right)e^2 v_b\gamma_0 B_0\left(\hat{\rho}-i\hat{\varphi}\right)}{m_e\omega_0^{'}}e^{i(\delta-\varphi)}e^{-i\left(\omega_s\left(t-\frac{r}{c}\right)\right)}\frac{e^{i\left(\frac{\omega}{v_b}-\frac{\omega_s\cos\theta}{c}+k_0^{'}\right)L_b}-1}{i\left(\frac{\omega}{v_b}-\frac{\omega_s\cos\theta}{c}+k_0^{'}\right)}$$

The Magnetic field of THz radiation is

$$\vec{B}=\Delta\times\vec{A}\approx\left(i\frac{\omega_s}{c}\right)\hat{\rho}\times\vec{A} \qquad (19)$$

Substitute the value of $\vec{A}$ in Eq.(19), we get

$$\vec{B}=\left(i\frac{\omega_s}{c}\right)\hat{\rho}\times\left(\hat{\rho}-i\hat{\varphi}\right)\frac{\mu_0 r_b^2}{r}\frac{2n_b J_1\left(\frac{\omega L\psi}{v_b}\right)e^2 v_b\gamma_0 B_0}{m_e\omega_0{}'}e^{i(\delta-\varphi)}e^{-i\left(\omega_s\left(t-\frac{r}{c}\right)\right)}\frac{e^{i\left(\frac{\omega}{v_b}-\frac{\omega_s\cos\theta}{c}+k_0'\right)L_b}-1}{i\left(\frac{\omega}{v_b}-\frac{\omega_s\cos\theta}{c}+k_0'\right)}$$

$$\vec{B}=\left(i\frac{\omega_s}{c}\right)\left(-i\hat{z}\right)\frac{\mu_0 r_b^2}{r}\frac{2n_b J_1\left(\frac{\omega L\psi}{v_b}\right)e^2 v_b\gamma_0 B_0}{m_e\omega_0{}'}e^{i(\delta-\varphi)}e^{-i\left(\omega_s\left(t-\frac{r}{c}\right)\right)}\frac{e^{i\left(\frac{\omega}{v_b}-\frac{\omega_s\cos\theta}{c}+k_0'\right)L_b}-1}{i\left(\frac{\omega}{v_b}-\frac{\omega_s\cos\theta}{c}+k_0'\right)}$$

Let $M=\dfrac{e^{i\left(\frac{\omega}{v_b}-\frac{\omega_s\cos\theta}{c}+k_0'\right)L_b}-1}{i\left(\frac{\omega}{v_b}-\frac{\omega_s\cos\theta}{c}+k_0'\right)}\dfrac{L_b/2}{L_b/2}$

Let $\theta_1=\left(\frac{\omega}{v_b}-\frac{\omega_s\cos\theta}{c}+k_0'\right)\frac{L_b}{2}$

Now M will become-

$$M=e^{i\theta_1}\left(\frac{e^{i\theta_1}-e^{-i\theta_1}}{i\theta_1}\right)\frac{L_b}{2}$$

$$M=\frac{e^{i\theta_1}}{\theta_1}L_b\sin\theta_1$$

Expression of magnetic field reduces to-

$$\vec{B}=\left(\frac{\omega_s}{c}\right)\frac{\mu_0 r_b^2}{r}\frac{2n_{bo}J_1\left(\frac{\omega L\psi}{v_b}\right)e^2 v_b\gamma_0 B_0}{m_e\omega_0{}'}e^{i(\delta-\varphi)}e^{-i\left(\omega_s\left(t-\frac{r}{c}\right)\right)}\frac{e^{i\theta_1}}{\theta_1}L_b\sin\theta_1\hat{z}$$

By taking mode and squaring above expression-

$$\left|\vec{B}\right|^2 = \frac{\omega_s^2}{c^2}\frac{\mu_0^2 r_b^4}{r^2}\frac{4n_b^2 J_1^2\left(\frac{\omega L\psi}{v_b}\right)e^4 v_b^2\gamma_0^2 B_0^2}{m_e^2\omega_0^{'2}}L_b^2\frac{\sin^2\theta_1}{\theta_1^2} \tag{20}$$

Time average pointing vector is given by

$$\vec{P}_{avg} = \hat{r}\frac{c}{2\mu_0}\left|\vec{B}\right|^2 \tag{21}$$

Substitute the value of $\left|\vec{B}\right|^2$ from Eq. (20) in Eq. (21), we get

$$\vec{P}_{avg} = \hat{r}\frac{c}{2\mu_0}\frac{\omega_s^2}{c^2}\frac{\mu_0^2 r_b^4}{r^2}\frac{4n_b^2 J_1^2\left(\frac{\omega L\psi}{v_b}\right)e^4 v_b^2\gamma_0^2 B_0^2}{m_e^2\omega_0^{'2}}L_b^2\frac{\sin^2\theta_1}{\theta_1^2}$$

$$\vec{P}_{avg} = \hat{r}\frac{4R_b^4}{K_0^2}\frac{\omega_s^2}{\omega_{01}^2}\frac{\omega_b^4}{\omega_{01}^4}\frac{L_b^2}{r^2}\frac{\sin^2\theta_1}{\theta_1^2}J_1^2\left(\frac{\omega L\psi}{v_b}\right)\times cB_0^2/2\mu_0$$

$$\vec{P}_{avg} = \hat{r}\frac{4R_b^4}{K_0^2}\frac{\omega_s^2}{\omega_{01}^2}\frac{\omega_b^4}{\omega_{01}^4}\frac{L_b^2}{r^2}\frac{\sin^2\theta_1}{\theta_1^2}J_1^2\left(\frac{\omega^2}{\omega_{01}^2}A\right)\times cB_0^2/2\mu_0$$

where $A = \frac{1}{2\gamma_0^4}\frac{\omega_{01}d}{c}\frac{\omega_{01}L}{c}\frac{c^3}{v_b^3}\frac{eA_1}{m_e\omega_{01}c}\frac{eA_2^*}{m_e\omega_{01}c}\frac{\sin\left(\theta_g\right)}{\theta_g}$

$R_b = \frac{r_b\omega_{01}}{c}$, $K_0 = \frac{ck_0}{\omega_{01}}$, $\omega_b^4 = \frac{n_b^2 e^4}{m_e^2\varepsilon_0^2}$ and $\frac{\omega L\psi}{v_b} = \frac{\omega^2}{\omega_{01}^2}A$

3.4 Amplitude of THz Wave

Wave equation for THz wave is

$$\nabla^2\vec{E}_\omega+\frac{1}{c^2}\frac{\partial^2\vec{E}_\omega}{\partial t^2}=\frac{-i\omega_s}{c^2\varepsilon_0}\vec{J}_\omega^{NL} \tag{22}$$

Let $\vec{E}_\omega=\hat{x}A_\omega(z)e^{-i(\omega_s t-K_{THZ}z)}$,

where $K_{THZ}=\frac{\omega}{v_b}+k_0^{'}$

By Substituting value of $\vec{E}_\omega$ and $\vec{J}_\omega^{NL}$ in Eq. (22), we get

$$\nabla^2\vec{E}_\omega+\frac{1}{c^2}\frac{\partial^2\vec{E}_\omega}{\partial t^2}=\frac{-i\omega_s}{c^2\varepsilon_0}\frac{2n_bJ_1\left(\frac{\omega L\psi}{v_b}\right)e^2v_b\gamma_0B_0(\hat{\rho}-i\hat{\varphi})}{m_e\omega_0^{'}}e^{-i\left[\omega_s t-\left(\frac{\omega}{v_b}+k_0^{'}\right)z^{'}\right]}$$

$$2iK_{THZ}\frac{\partial A_\omega}{\partial z}+2iK_{THZ}\frac{\partial A_\omega}{\partial t}+\left(-K_{THZ}^2+\frac{\omega^2}{c^2}\right)A_\omega=\frac{-i\omega_s}{c^2\varepsilon_0}\frac{2n_bJ_1\left(\frac{\omega L\psi}{v_b}\right)e^2v_b\gamma_0B_0(\hat{\rho}-i\hat{\varphi})}{m_e\omega_0^{'}}\times e^{-i\left[\omega_s t-\left(\frac{\omega}{v_b}+k_0^{'}\right)z^{'}\right]}$$

At exact phase matching condition third term on left hand side becomes zero and $\frac{\partial A_\omega}{\partial t}$ also vanishes.(A_ω is the amplitude not varying with time).

So above Eq. reduces to-

$$\frac{\partial A_\omega}{\partial z}=\frac{-i\omega_s}{c^2\varepsilon_0}\frac{2n_bJ_1\left(\frac{\omega L\psi}{v_b}\right)e^2v_{bo}\gamma_0B_0(\hat{\rho}-i\hat{\varphi})}{m_e\omega_0^{'}2iK_{THZ}}$$

$$\frac{\partial A_\omega}{\partial z}=\frac{-i\omega_s}{c^2\varepsilon_0}\frac{2n_bJ_1\left(\frac{\omega L\psi}{v_{bo}}\right)e^2v_b\gamma_0B_0(\hat{\rho}-i\hat{\varphi})}{m_e\gamma_0k_0v_b2iK_{THZ}}$$

$$\frac{\partial A_\omega}{\partial z} = \frac{-i\omega_s}{c^2\varepsilon_0}\frac{2n_b J_1\left(\frac{\omega L\psi}{v_b}\right)e^2 B_0\left(\hat{\rho}-i\hat{\varphi}\right)}{m_e k_0 2iK_{THZ}}$$

$$\frac{\partial A_\omega}{\partial z} = \frac{-\omega_s}{c^2\varepsilon_0}\frac{n_b J_1\left(\frac{\omega L\psi}{v_{bo}}\right)e^2 B_0\left(\hat{\rho}-i\hat{\varphi}\right)}{m_e k_0 K_{THZ}}$$

$$\frac{\partial A_\omega}{\partial z} = \frac{-\omega_s}{c^2}\frac{\omega_b^2 B_0\left(\hat{\rho}-i\hat{\varphi}\right)}{k_0 K_{THZ}} J_1\left(\frac{\omega L\psi}{v_b}\right)$$

$$A_\omega = \int_0^{L_w} \frac{-\omega_s}{c^2}\frac{\omega_b^2 B_0\left(\hat{\rho}-i\hat{\varphi}\right)}{k_0 K_{THZ}} J_1\left(\frac{\omega L\psi}{v_b}\right)dz$$

$$A_\omega = \frac{-\omega_s}{c^2}\frac{\omega_b^2 L_w B_0\left(\hat{\rho}-i\hat{\varphi}\right)}{k_0 K_{THZ}} J_1\left(\frac{\omega L\psi}{v_b}\right)$$

$$\left|A_\omega\right| = \frac{1}{K_0}\frac{\omega_s}{\omega}\frac{\omega_b^2}{\omega_{01}^2}\frac{\omega_{01}L_b}{c}\frac{v_b}{c}\frac{L_w}{L_b}\frac{\omega_{01}}{\omega}\left(1+\frac{K_0 v_b}{c}\frac{\omega_{01}}{\omega}\right)^{-1} J_1\left(\frac{\omega^2}{\omega_{01}^2}A\right)$$

$$\left|A_\omega\right|^2 = \frac{1}{K_0^2}\frac{\omega_s^2}{\omega^2}\frac{\omega_b^4}{\omega_{01}^4}\frac{\omega_{01}^2 L_b^2}{c^2}\frac{v_b^2}{c^2}\frac{L_w^2}{L_b^2}\frac{\omega_{01}^2}{\omega^2}\left(1+\frac{K_0 v_b}{c}\frac{\omega_{01}}{\omega}\right)^{-2} J_1^2\left(\frac{\omega^2}{\omega_{01}^2}A\right)$$

where $K_0 = \frac{ck_0}{\omega_{01}}$, $\omega_b^4 = \frac{n_b^2 e^4}{m_e^2 \varepsilon_0^2}$

Chapter 4

Results

4.1 Results

Laser bunched electron beam coupling to a helical wiggler appears a potential candidate for THz generation. THz power scales as square of bunch radius and beam current, linearly with bunch length, and inverse square of wiggler wave vector. For a fixed drift space length L, the THz power increases with THz frequency, attains a maximum at ω =2.7 THz, for beam velocity $v_b = 0.94c$ and then falls off due to the Bessel function character of density modulation. The frequency of the THz radiation can be tuned by the changes in the wavelengths of the lasers. The power conversion efficiency from the beam to THz can be of the order of a percent. One may note that the length of the modulator segment could be fairly large as compared to the THz wavelength as the beam travels with a velocity close to the phase velocity of the ponderomotive force. However, we neglect this effect which may be as long as Lw < L. We have ignored the beam space charge effect that may be justified as long as the growth rate exceeds the beam plasma frequency.

Parameters of electron beam and helical wiggler are given in Table 4.1.

We have carried numerical calculations of THz power and amplitude for the following parameters: $\omega_1 L/c$=7× 10^4, $\omega_1 d/c$=2× 10^3,$\gamma_0 = 2.93, R_b 1950, \omega_b/\omega_1$=7. 98 × 10^{-6}, $K_0 = 3.768\times10^{-3}$. We have plotted the THz power with ω/ω_1 for different values of beam velocity $v_b = 0.94c$ in Fig. 4.1. Initially, THz power increases with frequency and attains a maximum value 3.9×10^{11} watt/m^2 at ω=2.7 THz and then falls off.

.

Table 4.1 Parameters used in THz Generation

Electron beam energy	1Mev
Electron beam size	r_b =5.85 mm
Electron beam density	$n_b = 10^{15}/m^3$
Velocity of beam	v_b =0.94c
Wavelength for Laser 1	$\lambda_1 = 3\mu m$
Wavelength for Laser 2	$\lambda_2 = 3(1 + \lambda_1/\lambda_{THz})$
Length of modulator	d=6mm
Length of Drift space	L=20 cm
Length of wiggler	$L_w = 5m$
Electron bunch length	$L_b = 0.5cm$
Wiggler wavelength	$\lambda_w = 5mm$
Magnetic Flux Density	Bo=0.85 T

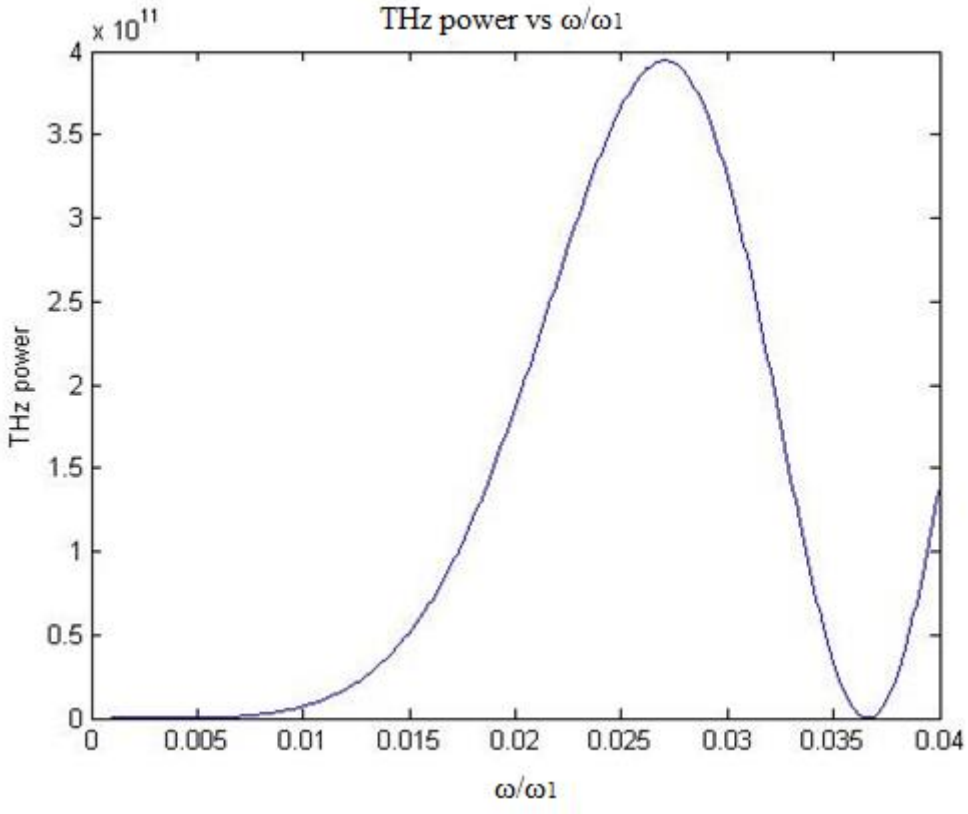

Figure 4.1 THz Power as a function of ω/ω_1 for v_b/c =0.94

Figure 4.2 shows the variation of magnetic flux density of Helical wiggler with THz power. THz power varies as square of magnetic flux density. We have plotted the magnetic flux density for ω/ω_1=0.027 and $v_b = 0.94c$

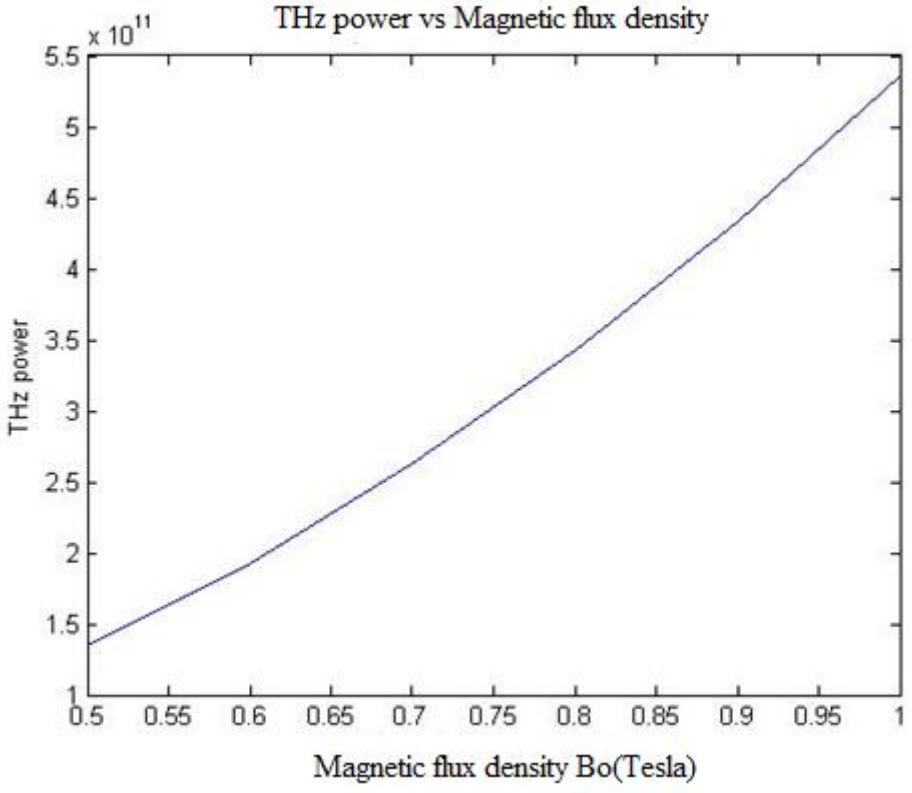

Figure 4.2 THz power variation with Magnetic flux density B_0 of Helical wiggler

Figure 4.3 shows the variation of wiggler wavelength with THz power. THz power varies as square of wiggler wavelength as shown. We have plotted THz power with the wiggler wavelength for ω/ω_1=0.027 and $v_b = 0.94c$

Figure 4.4 shows the variation of THz amplitude with ω/ω_1 for the beam velocity $v_b = 0.94c$. THz amplitude increases with THz frequency to a maximum value and then falls off due to the Bessel function character of density modulation.

Figure 4.5 shows the graph of THz amplitude varies with length of helical wiggler at 2.5 THz frequency for the beam velocity $v_b = 0.94c$. THz amplitude is proportional to the length of helical wiggler.

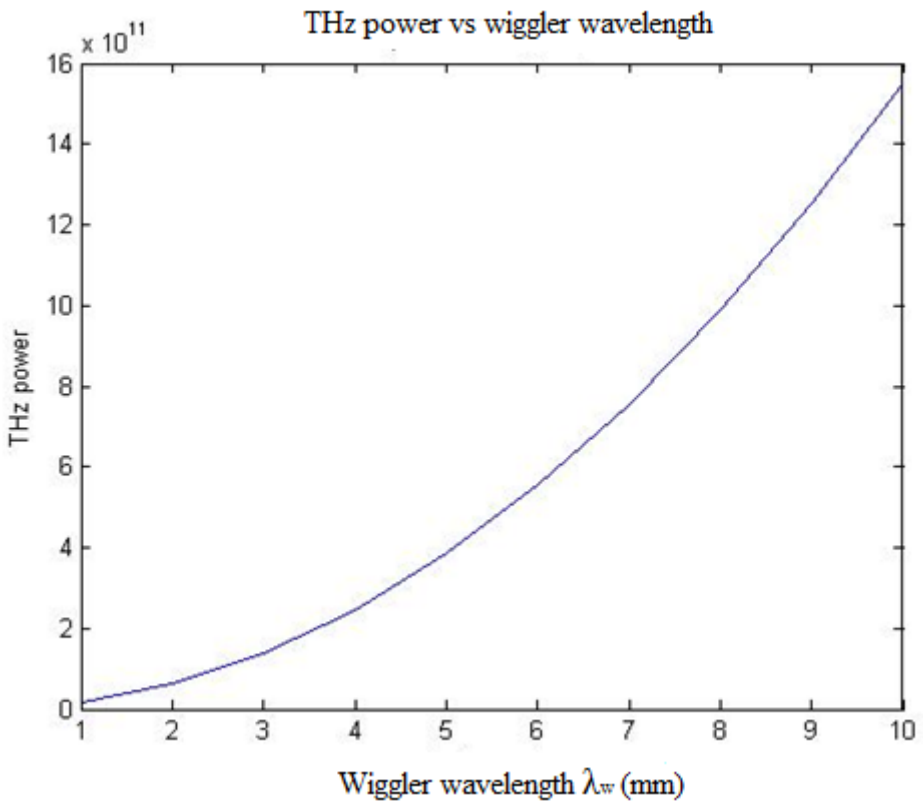

Figure 4.3 THz power variation with Wiggler wavelength λ_w for ω/ω_1=0.027

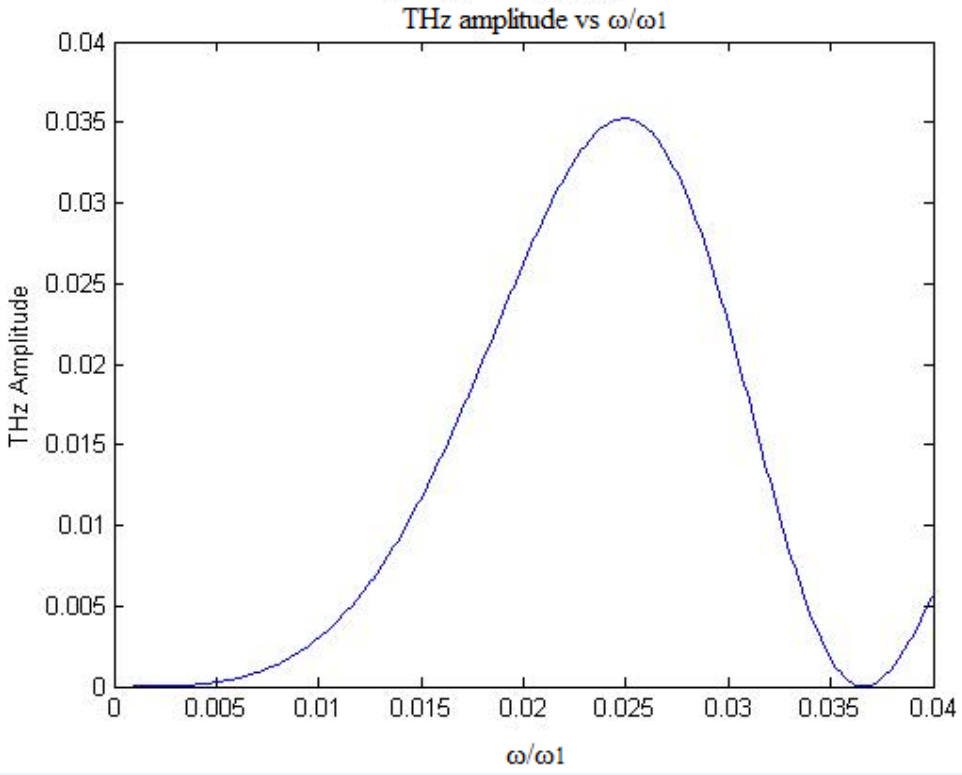

Figure 4.4 THz Amplitude as a function of ω/ω_1 for v_b/c=0.94

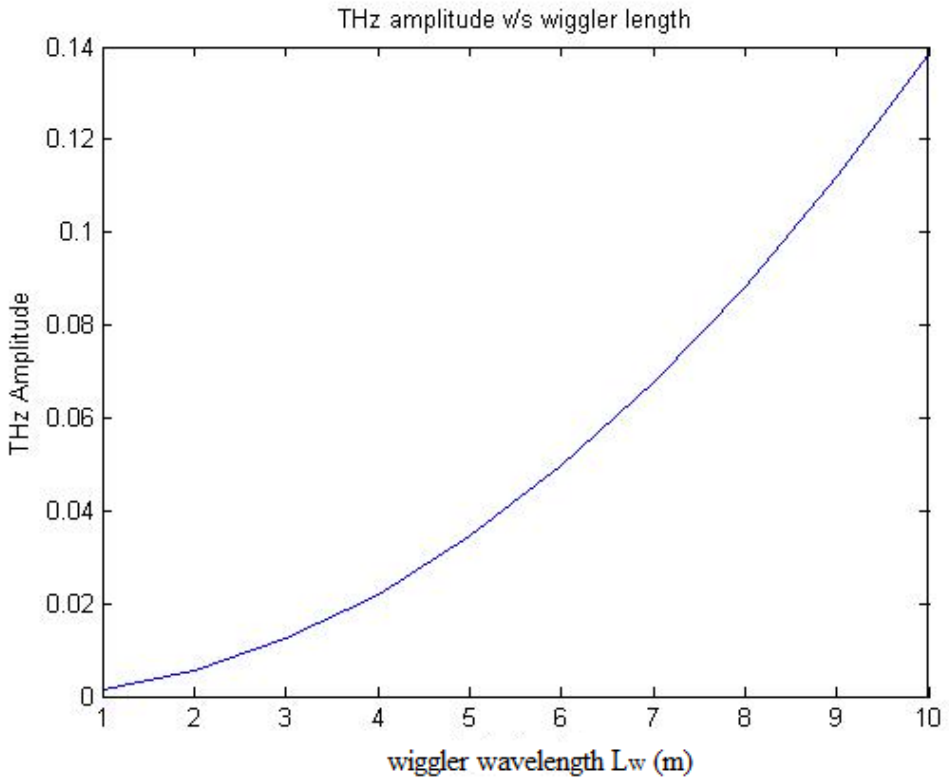

Figure 4.5 THz Amplitude variation with wiggler length L_w

The variation of THz power with bunching factor is shown in figure 4.6 which shows the characteristic of sinc function. It will attain maximum value at origin and decreases as bunching factor increases.

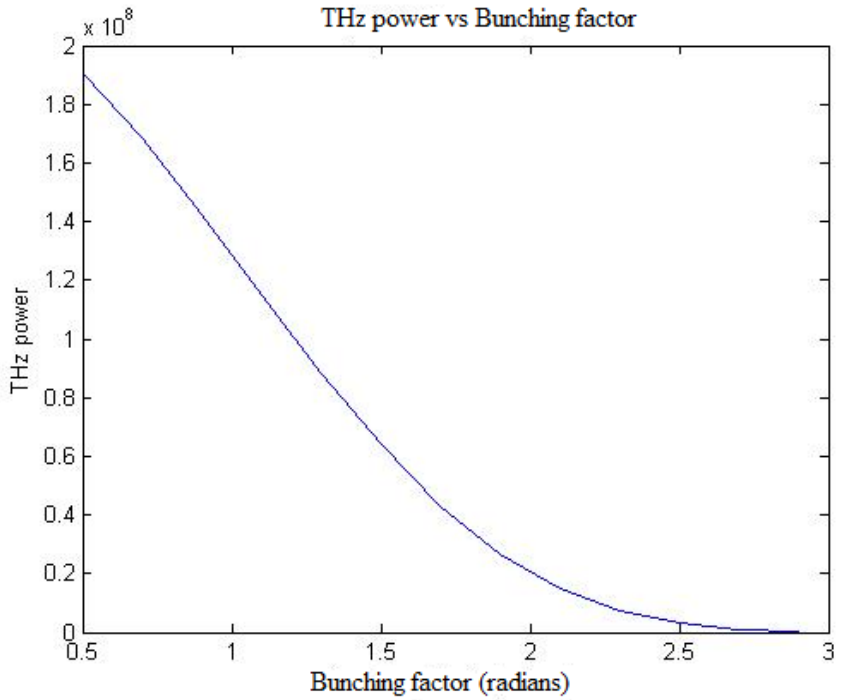

Figure 4.6 THz power variation with bunching factor (radians)

4.2 Role of Helical wiggler

The mathematical expression of THz radiation generation is derived. Different parameters of Helical wiggler are plotted with THz power and THz amplitude. Magnetic flux density B_0 of Helical wiggler scales as square with THz power i.e. with increase in magnetic flux density B_0 , THz power increases. Helical wiggler wavelength λ_w (wiggler period) also varies as square with THz power.

The length of Helical wiggler L_w varies as square with square of THz amplitude i.e. Length of wiggler is proportional to THz amplitude, with increase in length of wiggler intensity of FEL increases.

REFERENCE

[1] B. Ferguson and X. C. Zhang. Materials for Terahertz Science and Technology. *Nature Materials* 1(1):26–33, 2002.

[2] J. S. E. Knoesel, M. Bonn and T. F. Heinz, "Charge transport and carrier dynamics in liquids probed by Thz time-domain spectroscopy," *Phys. Rev. Lett.*, vol. 86, pp. 340–343,Jan. 2001.

[3] G. M. H. Knippels, X. Yan, A. M. Macleod, W. A. Gillespie, M. Yasumoto, D. Oepts, and A. F. G. van der Meer, "Generation and complete electric-field characterization of intense ultrashort tunable far-infrared laser pulses," *Phys. Rev. Lett.*, vol. 83, pp. 1578–1581, 1999.

[4] S. Park, A. M. Weiner, M. R. Melloch, C. W. Siders, J. L. W. Siders, and A. J. Taylor, "High-power narrow-band terahertz generation using large-aperture photoconductors," *IEEE J. Quantum Electron.*, vol. 35, no. 8, pp. 1257–1268, Aug. 1999.

[5] K. Yang, P. Richards, and Y. Shen, "Generation of far-infrared radiation by picosecond light pulses in LiNbO3," *Appl. Phy. Lett.*, vol. 19, pp. 320–323, Nov. 1971.

[6] M. Joffre, A. Bonvalet, A. Migus, and J.-L. Martin, "Femtosecond diffracting fourier-transform infrared interferometer," *Opt. Express*, vol. 21, pp. 964–966, 1996.

[7] Renbo Song, Wei Shi, and Y. J. Ding. Direct measurements of resonance peaks of DNA and proteins using widely tunable monochromatic THz source. Volume vol.1 of *2003 IEEE LEOS Annual Meeting Conference Proceedings (IEEE Cat. No.03CH37460)*, page 238 vol.1, Piscataway, NJ, USA, 2003. IEEE.

[8] Yun-Shik Lee. *Principles of Terahertz Science and Technology*. Springer Publishing Company, Incorporated, 2008.

[9] X. D. Mu, I. B. Zotova, and Y. J. Ding. Power scaling on efficient generation of ultrafast terahertz pulses. *IEEE Journal of Selected Topics in Quantum Electronics*, 14(2): 315–332,2008.

[10] Xu Xie, Jianming Dai, and X. C. Zhang. Coherent control of thz wave generation in ambient air. *Phys. Rev. Lett.*, 96(7):075005, 2006. 110.

[11] W. Shi, Y. J. J. Ding, N. Fernelius, and K. Vodopyanov. Efficient, tunable, and coherent 0.18-5.27-THz source based on GaSe crystal. *Optics Letters*, 27(16):1454–1456, 2002.

[12] F. Capasso, K. Mohammed, and A. Y. Cho. Resonant tunneling through double barriers, perpendicular quantum transport phenomena in superlattices and their device application. *IEEE J. Quan. Electronics*, 22(9):1853–1869, 1986.

[13] J. Faist, F. Capasso, D. L. Sivco, C. Sirtori, A. L. Hutchinson, and A. Y. Cho.Quantum cascade laser. *Science*, 264(5158):553–556, 1994.

[14] J. Faist, F. Capasso, C. Sirtori, D. L. Sivco, J. N. Baillargeon, A. L. Hutchinson,S. N. G. Chu, and A. Y. Cho. High power mid-infrared quantum cascade lasers operating above room temperature. *Appl. Phys.Lett.*,68(26):3680–3682, 1996.

[15] R. Kohler, A. Tredicucci, F. Beltram, H. E. Beere, E. H. Linfield, A. G. Davies, D. A. Ritchie, R. C. Iotti, and F. Rossi. Terahertz semiconductor heterostructure laser. *Nature*, 417(6885):156–159, 2002.

[16] B. S. Williams, S. Kumar, Q. Hu, and J. L. Reno. Operation of Terahertz quantum-cascade lasers at 164 k in pulsed mode and at 117 k in continuous wave mode. *Optics Express*, 13(9):3331–3339, 2005.

[17] M. A. Belkin, F. Capasso, A. Belyanin, D. L. Sivco, A. Y. Cho, D. C. Oakley, C. J. Vineis, and G. W. Turner. Terahertz quantum-cascade-laser source based on intracavity difference-frequency generation. *Nature Photonics*, 1(5):288–292, 2007.

[18] Shur, M., "Terahertz Technology: Devices and applications," Proceedings of ESSCIRC, 13–21, Grenoble, France, 2005.

[19] Goyette, T. M., A. Gatesman, T. M. Horgan, et al., "THz compact range radar systems," Pennsylvania, June 13, 2003.

[20] Huang, Z.; Kim, K. J. (2007). "Review of x-ray free-electron laser theory". *Physical Review Special Topics - Accelerators and Beams* 10(3).

[21] "Duke University Free-Electron Laser Laboratory". Retrieved 2007-12-21.

[22] F. J. Duarte (Ed.), *Tunable Lasers Handbook* (Academic, New York, 1995) Chapter 9.

[23] "New Era of Research Begins as World's First Hard X-ray Laser Achieves "First Light"". SLAC National Accelerator Laboratory. April 21, 2009. Retrieved 2013-11-06.

[24] Hans Motz, W. Thon, R.N. Whitehurst, Experiments on radiation by fast electron beams, *J. Appl. Phys.*, 24(7):826-833, 1953.

[25] Motz, Hans (1951). "Applications of the Radiation from Fast Electron Beams". *J. Appl. Phys.*, 22 (5): 527. doi:10.1063/1.1700002.

[26] "Phys. Rev. Lett. 38, 892 (1977): First Operation of a Free-Electron Laser". Prl.aps.org. Retrieved 2014-02-17.

[27] Feldhaus, J.; Arthur, J.; Hastings, J. B. (2005). "X-ray free-electron lasers". *Journal of Physics B: Atomic, Molecular and Optical Physics* **38** (9): S799. doi:10.1088/0953 4075/38/9/023

[28] Manoj kumar, V.K. Tripathi, "Terahertz radiation from a laser bunched relativistic electron beam in a magnetic wiggler" *Phys. plasma* 19,073109(2012).